Journal Name

ARTICLE TYPE

Cite this: DOI: 10.1039/xxxxxxxxxx

Influence of interface stabilisers and surrounding aqueous phases on nematic liquid crystal shells†

JungHyun Noh, Kevin Reguengo De Sousa, and Jan P. F. Lagerwall*

Received Date
Accepted Date

DOI: 10.1039/xxxxxxxxxx

www.rsc.org/journalname

We investigate the nematic-isotropic (N-I) transition in shells of the liquid crystal 5CB, surrounded by aqueous phases that conventionally are considered to be immiscible with 5CB. The aqueous phases contain either sodium dodecyl sulfate (SDS) or polyvinyl alcohol (PVA) as stabiliser, the former additionally promoting homeotropic director alignment. For all shell configurations we find a depression of the clearing point compared to pure 5CB, indicating that a non-negligible fraction of the constituents of the surrounding phases enter the shell, predominantly water. In hybrid-aligned shells, with planar outer and homeotropic inner boundary (or vice versa), the N-I transition splits into two steps, with a consequent three-step textural transformation. We explain this as a result of the order-enhancing effect of a monolayer of radially aligned SDS molecules adsorbed at the homeotropic interface.

During recent years there has been an increasing interest in the effects of topological constraints on liquid crystals with curved boundaries, to a large extent focusing on thin shells produced by a microfluidic technique.[1] A thin layer of liquid crystal is confined between two isotropic liquids that are generally considered to be immiscible with the liquid crystal. One forms an internal droplet, the other provides the external continuous phase in which the shells are suspended. After the initial report by Fernandez-Nieves et al.[2] on the configurations of topological defects in planar-aligned nematic shells, several experimental studies have focused on the impact of shell thickness,[3] homeotropic[4] and hybrid[5,6] alignment, nematic—smectic A[4,7] and smectic A—smectic C[8] phase transitions, chiral nematic shells and droplets,[9–13], shells loaded with microparticles,[14] as well as nematic shells polymerised into liquid crystal elastomer actuators[15]. In parallel with this development a number of theoretical and simulation studies have helped to further develop a detailed picture of liquid crystalline ordering processes in nematic and smectic shells.[16–21]

Surprisingly, little attention has been devoted to the nematic-isotropic (clearing) transition in the shell. Likewise, the influence of the surrounding liquid phases and the interface stabilisers, playing a critical dual role in preventing shell collapse and ensuring the desired liquid crystal alignment, has been largely neglected. Here we investigate the clearing transition in nematic shells of the commonly studied liquid crystal 4-Cyano-4'-n-pentylbiphenyl (5CB, Synthon Chemicals, Germany) surrounded by isotropic aqueous phases of different compositions. The shells are stabilized by polyvinyl alcohol (PVA, M_w 13,000 - 23,000 g mol^{-1}, 87-88% hydrolysed, Sigma-Aldrich) at interfaces where planar alignment is desired, or by sodium dodecyl sulfate (SDS, Sigma-Aldrich) for homeotropic alignment. By systematically interchanging SDS and PVA in the internal and external phases, by varying their respective concentrations, and by using either pure water or a water-glycerol mixture as isotropic solvent, we find an unexpectedly rich set of scenarios. At the same time we develop a deeper understanding of how the liquid crystal is affected by the composition of the surrounding phases. We conclude that water enters the liquid crystal to a sufficient degree to reduce the 5CB clearing point, SDS and glycerol also going into or through the shell to some extent. Moreover, while PVA can be considered a passive stabiliser, the planar alignment resulting from direct contact between the 5CB and aqueous phases,[22] an adsorbed monolayer of SDS molecules not only stabilizes the shell and aligns the director, it can also locally enhance the nematic order.

We produce the liquid crystal shells using a glass capillary microfluidic set-up, following the design developed by Weitz and co-workers.[23] 5CB and a co-flowing aqueous inner fluid are flow-focused by the outer aqueous phase, causing the liquid crystal to be encapsulated between the inner and outer fluids. In most of

University of Luxembourg, Physics & Materials Science Research Unit, 162a Avenue de la Faiencerie, Luxembourg, Luxembourg. Fax: +352 46664436219; Tel: +352 4666446219; E-mail: jan.lagerwall@lcsoftmatter.com

† Electronic Supplementary Information (ESI) available: complementary details on the N-I transition in hybrid shells; director field at very low surfactant concentration; movies of N-I transition in shells with homeotropic, planar and hybrid alignment, respectively, in the latter case viewed along as well as perpendicular to gravity. See DOI: 10.1039/b000000x/

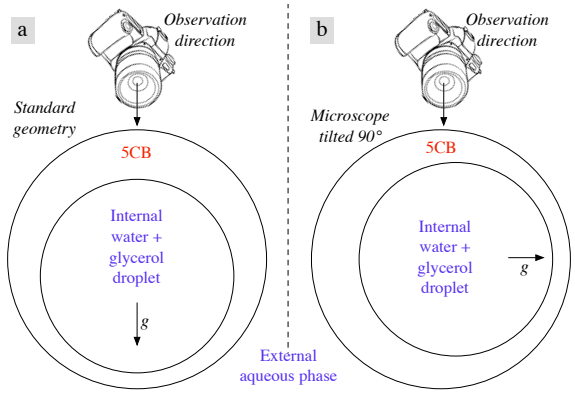

Fig. 1 Schematic drawing of the geometry of liquid crystal shells with WG inside, indicating the relative observation direction during normal experiments (a) as well as during experiments with 90° tilted microscope (b). The direction of gravity is indicated by the arrow labelled *g*.

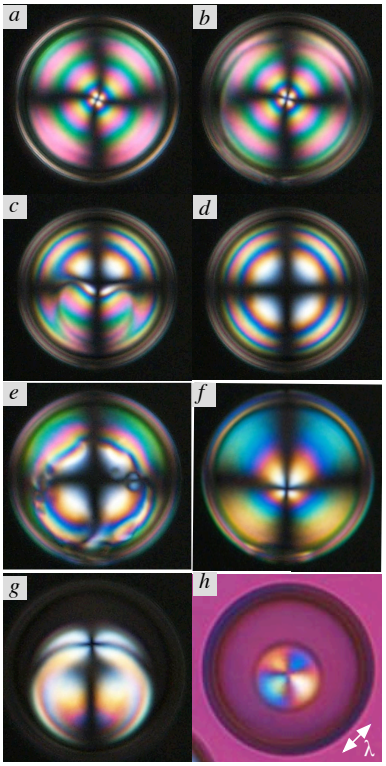

Fig. 2 (a-h) N-I transition in a hybrid-aligned shell, containing 1 wt.-% PVA in the inner drop and 1 wt.-% SDS in the outer phase. The focus is on the thicker part of the shell. In (h) the optic axis orientation of the inserted first-order phase plate is indicated by the white arrow labeled λ.

our experiments these are both based on a water+glycerol mixture (50/50 volume ratio, corresponding to ∼56 wt.-% glycerol), in the following referred to as WG, as this results in convenient values of viscosity and density. For reference, a limited number of experiments were also conducted without addition of glycerol.

The shells are prepared with 100 - 150 μm diameter and thickness below 10 μm. Due to a lower density of 5CB than an internal WG droplet, the latter sinks towards the bottom of the shell. This renders the shell slightly asymmetric in thickness, the bottom being the thinnest part, cf. Fig. 1a. After production, the shells are collected in a bath filled with the outer continuous phase and transferred into a rectangular glass capillary for optical microscopy investigation. The sample is placed on a hot stage (Linkam Scientific Instruments, T95-PE) mounted on a polarising optical microscope (Olympus BX-51, Japan).

Our initial experiments were carried out with hybrid-aligned shells, prepared with 1 wt.-% of PVA in the inner WG droplet and 1 wt.-% of SDS in the outer continuous WG phase. As required by topology,[1] the planar PVA-stabilized inside features surface defects that together produce a total topological charge of +2. The director bend from planar inside to homeotropic outside breaks the director sign invariance and thus rules out non-integer defects,[5] leaving two +1 surface defects at the bottom and top of the shell inside, respectively.[6] The top defect is pictured in Fig 2a, at the core of a slightly inclined Maltese cross at the center of the photo. Upon heating at 0.01 K/min, we recognised the start of the clearing transition at $T_{NI}^1 = 34.8$°C through a ring rising from the bottom to the top of the shell, cf. Fig. 2b and Movie 1 in the ESI. While moving upwards, the ring expands to the perimeter and then shrinks towards the center, cf. Fig. 2c. In the process it is deformed and the texture eventually stabilizes into a distinctly different pattern, cf. Fig. 2d, which stays unchanged for several minutes of continued heating at this slow rate. The new texture, identical to the classic conoscopy texture of a homeotropic-aligned flat nematic, is a signature of homeotropic shell alignment,[4] hence we come to the surprising conclusion that the clearing transition in the initially hybrid-aligned shell is divided into two steps. These are separated by an intermediate state in which the shell is still (partially) nematic, with homeotropic alignment.

On continued heating, no further change is seen for another 0.05 K. The texture then appears to 'melt' at this T_{NI}^2, cf. Fig. 2e, again starting from the bottom of the shell. A highly deformed ring appears around the perimeter, shrinking towards the centre upon continued heating, bringing with it a second major texture change. A new Maltese cross forms, signifying the presence of a +1 surface defect at the centre of the picture, cf. Fig. 2f. The nematic phase then shrinks from the perimeter, as the shell finally turns fully isotropic. The +1 defect stays until the end of the transition, cf. Fig. 2g-h. Around the defect, the projection of the director field within the image plane is radial, as confirmed by inserting a first-order λ plate, cf. Fig. 2h.

To corroborate that the phase transition always nucleates at the thinnest part of the shell we repeated the experiment with the entire set-up tilted by 90°, such that the camera mounted on the microscope showed the shell from the side instead, gravity defining the vertical direction (geometry of Fig. 1b), cf. Movie 2 and Fig. 1 in the ESI. The transition could now be followed in full detail, confirming that both steps of the transition started at the thinnest and ended in the thickest point of the shell. The director field is maximally distorted around the defect located at the thinnest point in the shell, and one cannot rule out that this may play a role in nucleating the initial clearing transition at this point. However, the fact that also the second step, starting from a defect-free director configuration, also starts at the thinnest part

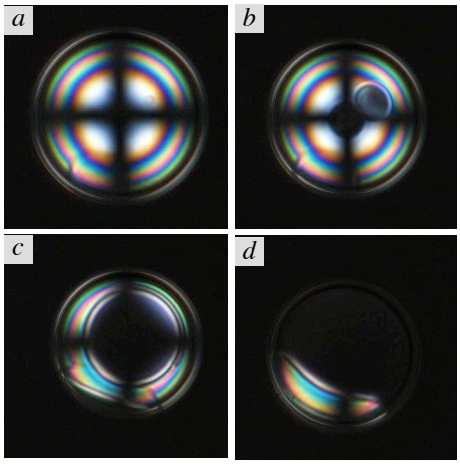

Fig. 3 N-I transition in a homeotropic-aligned shell, focused on the thinner bottom side. A characteristic homeotropic texture appears in (a) with a large cross and concentric rings. The start of the transition is seen at the thinner side of the shell (b). The nematic turns to isotropic phase via nucleated isotropic domains that expand and merge, in (c-d).

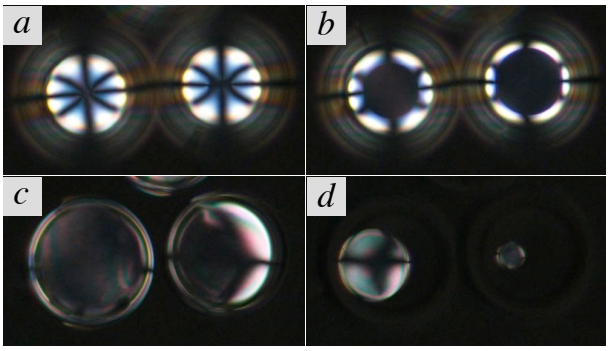

Fig. 4 N-I transition in planar-aligned shells, focused on the thinner bottom side where topological defects are located (a). The transition starts at the bottom (b), and then the phase boundary moves upwards, reaching the perimeter (c), and finally the top (d).

of the shell suggests that spatial variations in director field distortion provide only a secondary influence. We believe that the origin of the sequence is primarily the greater amount of heat that must be delivered to induce the phase transition across the shell radius, as its thickness increases from the bottom to the top.

We also studied the phase transition in an inverted hybrid shell, with SDS on the inside and PVA on the outside, finding qualitatively the same transition behaviour, see ESI Fig. 2. A difference in the colour and pattern of the fully nematic texture reflects a predominantly planar alignment in the thicker part of the shell, increasing the effective birefringence and reducing its variations across the sample plane. This can be traced back to the inverted balance between homeotropic and planar boundaries, as discussed in detail in the ESI.

The unexpected two-step N-I transition is unique to the hybrid-aligned shell. To demonstrate this, we compare first with a fully homeotropic-aligned shell, stabilised by 1 wt.-% SDS in WG at the inner and outer shell interfaces, cf. Fig. 3 and Movie 3 in the ESI. Figure 3a shows a characteristic homeotropic texture[4] with a defect free nematic configuration. As the temperature has reached 34.7°C, we observe the phase transition, again initiated near the bottom of the shell but with several nucleation points, cf. Fig. 3b. The isotropic domains expand and start merging, cf. Fig 3c-d, and during that process we see the remaining nematic domain rapidly shrink into a smaller region, to minimise the nematic-isotropic interfacial area. Turning into a fully isotropic phase, no further change is observed, hence we have a single-step N-I phase transition in the fully homeotropic-aligned shell.

We change to planar alignment on both shell interfaces, using 1 wt.-% PVA as stabilisers in inside and outside WG phases, and again study the N-I transition, cf. Fig. 4 and ESI Movie 4. Topology again requires defects to form, with a total topological charge $+2$.[1] This time they all gather close to the thinnest point of the shell, either two $+1$ surface defects (seen on the left shell in Fig. 4a) or, more commonly, four half-integer line defects (right shell). As has been discussed in detail previously[2,3] this arrangement minimises the free energy. On heating at 0.01 K/min, we notice the start of the clearing transition at the bottom of the shell in Fig. 4b, just below 35.0°C. The isotropic phase enters as a circular area that appears black between crossed polarisers. As the isotropic area expands on further heating, the phase boundary rises towards the top of the shell, as confirmed by continuously adjusting the microscope focus. Fig. 4c shows the phase boundary when it has reached the perimeter, and then it moves to the top of the shell while shrinking the nematic domain, cf. Fig. 4d. Thus, the N-I transition in fully planar-aligned shells also takes place in one step.

The two-step clearing transition observed in shells with asymmetric boundary conditions can be explained as follows. We first note that the planar alignment on the inside is due to the direct contact with glycerol and water,[22] and not to the PVA. This polymer is present in a disordered random coil conformation in the low-concentration solutions used, and it can thus not influence the alignment of the nematic. Its purpose is solely to prevent collapse or merging of shells. In contrast, the SDS acts both as a shell stabiliser and an alignment agent, if its concentration is high enough to ensure a high degree of surface coverage (see discussion below). It promotes homeotropic 5CB alignment at the interface where it adsorbs, thanks to an oriented arrangement with polar head groups directed into the aqueous phase and non-polar chains penetrating more or less radially into the liquid crystal.

Importantly, in addition to aligning the liquid crystal, this oriented adsorption—which is largely independent of temperature—stabilises nematic order locally, even slightly above the bulk clearing point, as shown by Bahr.[24] Therefore, as we heat the shell past T_{NI}^1, where the 5CB in contact with the PVA solution turns isotropic, the liquid crystal on the other side of the shell still remains nematic thanks to the ordering influence of the dense adsorbed surfactant layer. It does not turn isotropic until the second clearing point, T_{NI}^2, is reached. This explains why the transition always starts on the planar-aligned shell boundary, and why the alignment at that point always becomes fully homeotropic.

If the increase in clearing point originates in ordering from the adsorbed SDS layer, one would intuitively expect that $T_{NI}^2 > T_{NI}^1 \approx$

$T_{NI}^0 = 35.4°C$, where the latter is the transition temperature of pure bulk 5CB. It turns out, however, that 5CB shells surrounded by aqueous isotropic phases *always* turn fully isotropic at a temperature lower than T_{NI}^0, regardless of which stabilisers are used. This indicates that one or several of the constituents of the surrounding isotropic liquid phases enter the 5CB shell, the contamination leading to a depression of T_{NI}. Nevertheless, the SDS adsorption still induces a *relative* increase in clearing point T_{NI}^2 in the vicinity of the SDS layer, compared to the clearing point T_{NI}^1 of the contaminated 5CB shell at an interface without surfactant.

To gain a deeper understanding of the influence of the aqueous phases in contact with 5CB, we studied the N-I transition under systematically varied compositions of inner and outer phases, for symmetric as well as for asymmetric shells. All experiments were conducted within 10 minutes of preparing the shells, and with five selected samples we repeated the investigation after several days delay, in order to assess the steady state behavior. In a first series, the inner WG drop always contained 1 wt.-% of PVA, while the outer continuous WG phase contained SDS at varying concentration (c_{SDS}). Representative textures from this experiment, obtained soon after shell preparation, are shown in Fig. 5. Interestingly, the low-temperature nematic texture at c_{SDS} well below the Critical Micelle Concentration (CMC), about 0.3 wt.-% (13 mM) for SDS in WG at 25°C,[25] is identical to that of the fully planar aligned shells, stabilised by PVA on both sides. As in Fig. 4a, we recognise, in the left column of Fig. 5a-b, closely spaced defects with total topological surface charge +2 near the shell bottom. For $c_{SDS} \approx CMC$ and higher, the expected hybrid texture appears with two +1 defects at the top and bottom of the shell, respectively, cf. Fig. 5c-g, left column. On heating the shells, the two-step texture transformation during the N-I phase transition, via an intermediate homeotropic state as observed during our initial experiment (Fig. 2), is seen for all studied values of c_{SDS}.

It is interesting to compare the behavior at the two lower values of c_{SDS} with reports by Bahr[24] and by Gupta and Abbott,[26] both studies of which dealt with the director field of 5CB confined between an aqueous surfactant solution and a strongly homeotropic-aligning interface (air[24] or solid[26]). They found a threshold concentration orders of magnitude lower than CMC for realignment from hybrid to fully homeotropic. This can be explained as a result of the nematic elasticity that promotes a uniform director field.[26] Our case represents the complementary geometry, as the other interface of the shell promotes *planar* alignment. Thus, the same liquid crystal elasticity favoring uniform director field explains why we need rather high c_{SDS}, in the vicinity of the CMC, to achieve hybrid alignment in Fig. 5.

The investigations of shells several days after preparation revealed that two possible steady states are possible, which one depending on whether SDS is present in the system or not. Three SDS-free samples were investigated, both sides of the 5CB shells being stabilized by PVA. In one case this was dissolved in pure water, in the other two in the WG mixture. The fully planar orientation of the 5CB shell was intact at equilibrium, as expected, but all three samples showed an increased depression of the clearing point compared to T_{NI} immediately after preparation, cf. Fig. 6. While it is known that the solubility of glycerol

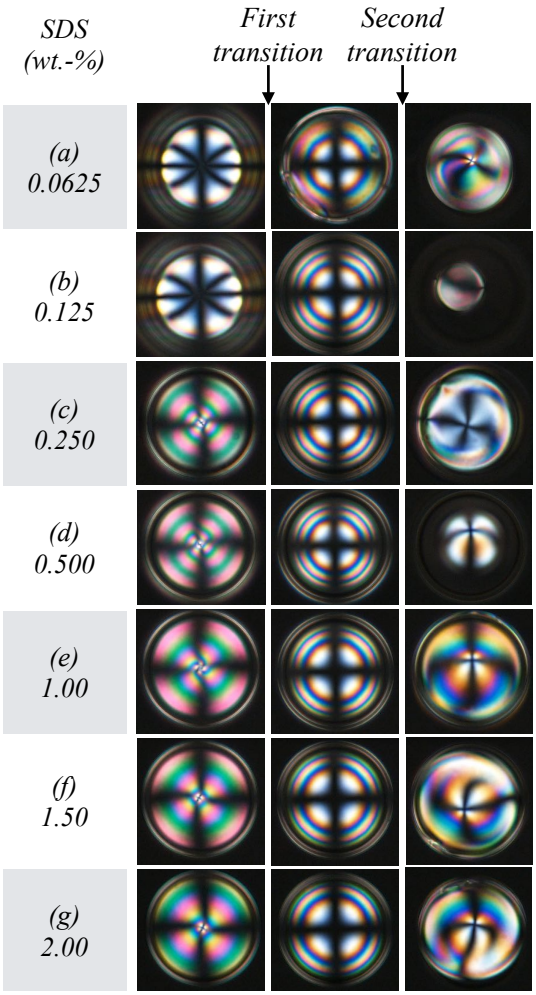

Fig. 5 N-I transition behaviour of hybrid shells, for varying SDS concentration (a-g). The first column shows low-temperature nematic textures. When the transition starts, a transformation into homeotropic texture takes place (middle column). On further heating, the fully isotropic state is reached via a second transition (third column).

in 5CB is non-negligible,[27] water is often considered immiscible with 5CB. However, the considerable reduction of the clearing point of the shell suspended between pure PVA-water solutions shows that water dissolves in 5CB at a concentration sufficient to affect the nematic phase stability. In fact, as is clear from the figure, the clearing point is actually higher—initially and at steady state—when 50% of the water has been replaced by glycerol, using the WG mixture. The solubility in 5CB of PVA can safely be considered fully negligible, due to its polymeric and hydrophilic nature. As almost all experimental work on liquid crystal shells is done with aqueous phases in contact with the liquid crystal, some contamination by water should be expected to be the norm.

The other two long-term experiments were conducted on samples where SDS was present in one or both aqueous phases (of WG type). Interestingly, the final alignment of *both* these samples was fully homeotropic, indicating that, in the former case, a considerable amount of surfactant had passed through the initially hybrid-aligned 5CB shells, from the SDS- to the PVA-stabilised

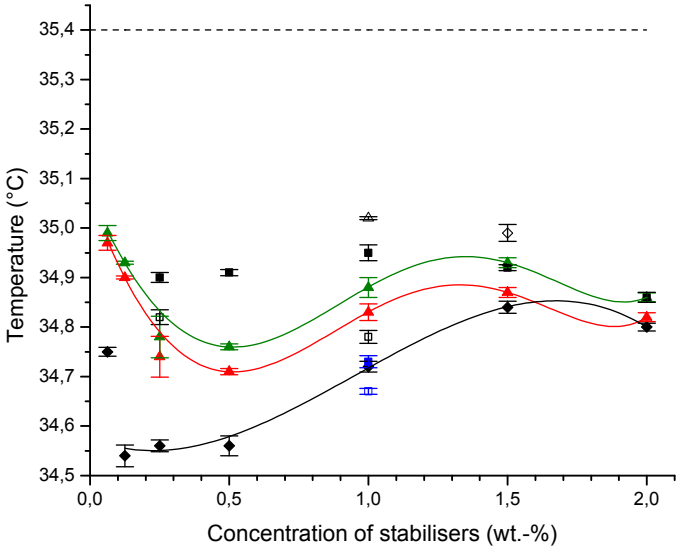

Fig. 6 N-I phase transition temperature as a function of stabiliser concentration in symmetric and asymmetric shells. The dashed horizontal line indicates the clearing point of pure 5CB. Symmetric PVA stabilization (giving fully planar alignment) is indicated with squares, symmetric SDS stabilization (normally giving homeotropic alignment) with diamonds, and asymmetric PVA/SDS boundary conditions (normally giving hybrid alignment) with triangles. In the latter case the internal phase always contains 1 wt.-% PVA, the x-axis referring to the SDS concentration in the outer continuous phase. Initial behavior is plotted with filled symbols, steady state behavior with empty symbols. Red and green data sets correspond to the first and second transition, respectively, seen in hybrid shells. The aqueous solvent was the WG mixture for all data points except the two blue ones, which were obtained with pure water as solvent for PVA.

side. Moreover, the shells in both samples were dramatically thinner than immediately after production, a result of the continuous removal of 5CB from the shell via encapsulation inside SDS micelles.[28] As a consequence, these exceptionally thin shells experienced the ordering influence of two very closely spaced monolayers of radially aligned SDS molecules, resulting in the highest clearing points seen in the study, cf. Fig. 6.

Coming to the behavior in symmetrically SDS-stabilized shells immediately after production, a surprising observation was that the lowest SDS concentration studied, $c_{SDS} = 0.0625$ wt-% (about 2.2 mM), gave rise to hybrid liquid crystal alignment, cf. ESI Fig. 4. Apparently, the interface coverage by SDS at this low concentration is so far from complete, that the anchoring energies for planar and homeotropic 5CB alignment are very similar. The slight increase in liquid crystal surface area on the shell outside is then sufficient to shift the balance in favor of planar alignment, while the shell inside has sufficient SDS coverage to be homeotropic. Further experiments to corroborate this conclusion are discussed in the ESI.

In connection to this change in alignment at low surfactant concentrations, it is illuminating that the lowest clearing points of the whole study are observed at c_{SDS} high enough to induce fully homeotropic liquid crystal alignment, but not much higher than CMC. With only 0.0625 wt-% SDS, yielding hybrid alignment, the clearing point was about 0.2 K higher directly after shell production. We believe that this difference is due to the anisotropic diffusion of a nematic phase:[29] water enters the liquid crystal shell much faster when it is homeotropically aligned than when one side is planar-aligned, where diffusion is slowed down as it must take place perpendicular to the director field. The diffusion into the shell is particularly fast when the SDS coverage of the homeotropic interface is incomplete, as expected below or in the vicinity of CMC. As more surfactant is added, the shell surfaces are essentially saturated with SDS molecules, limiting the direct access of water to the shell and thus explaining why the early-stage clearing point was found to increase for $c_{SDS} \geq 1$ wt.-%.

The slower diffusion of water through a planar-aligned liquid crystal interface is seen also by comparing the early-stage clearing points for planar-aligned shells with the corresponding final-state data. The trend is the opposite of the SDS-stabilized shells, with an initial clearing point that for shells suspended in PVA-loaded WG solutions is 0.1-0.2 K higher than the final clearing point, indicating that there was still a net inflow of water to the shells after the experiments on freshly produced shells were carried out. Also when pure water was used as PVA solvent the clearing point decreased from the initial to the final stage, but the change over time was smaller and already the initial T_{NI} was much lower than with the WG solution. The combination of glycerol and PVA thus seems to play an important role in slowing down the diffusion of water into the shells, possibly due to a weak gelation of adjacent PVA chains that can be triggered by strong hydrogen bonding with the three hydroxyl groups of each glycerol molecule.

As could be expected, the initial clearing points of the asymmetrically stabilized shells are largely intermediate between those of shells stabilized by only PVA and those stabilized by SDS alone, respectively, with the important addition, discussed above, that here we always detect two clearing points. Both of these reach their highest values when c_{SDS} is so low that the shell is fully planar-aligned, again confirming the importance of the liquid crystal alignment for the speed of diffusion of water into the shell.

The dissolution of water into 5CB may appear surprising, since thermotropic liquid crystals are often considered to be oil-like, but the polar cyano group and the two aromatic rings actually makes a 5CB molecule a much better hydrogen bonding partner for water than regular alkanes. Also SDS enters the shell, as is obvious from the long-term experiments on shells prepared with initially asymmetric PVA/SDS boundary conditions. The change over time from hybrid to fully homeotropic requires that SDS passes through the shell, but the final concentration of SDS inside the liquid crystal (thus not counting the surface-adsorbed monolayer) is probably very small.

In summary, we have demonstrated that the constituents of the aqueous isotropic phases that surround liquid crystal shells can drastically influence, not only the alignment, but also the temperature range of the nematic state, in non-trivial ways. Water enters the 5CB to a sufficient degree that the clearing point is clearly depressed. When glycerol and SDS are present, these components also enter, but the main part of the shift in T_{NI} is caused by water alone. While the steady state concentration of SDS molecules within the shell is probably negligible, they can

pass through the shell, turning an initially hybrid-aligned shell fully homeotropic on the time scale of days. Moreover, in addition to inducing homeotropic order if the SDS concentration is high enough to ensure sufficient surface coverage, the adsorbed oriented monolayer of SDS also stabilises the nematic order locally. As a consequence, a two-step clearing transition with intermediate alignment change is observed in hybrid shells, with surfactant-induced homeotropic orientation on one side and planar on the other. Planar alignment results due to the interaction with the water and/or glycerol when the bounding aqueous phase contains no or very low concentration of surfactant.

We thank Dr. Dirk Blunk and Dr. Christophe Blanc for helpful discussions. Support from the Fonds National de la Recherche Luxembourg, PhD Grant 6992111, is gratefully acknowledged.

References

1 T. Lopez-Leon and A. Fernandez-Nieves, *Colloid Polym. Sci.*, 2011, **289**, 345–359.
2 A. Fernandez-Nieves, V. Vitelli, A. Utada, D. R. Link, M. Marquez, D. R. Nelson and D. A. Weitz, *Phys. Rev. Lett.*, 2007, **99**, 157801.
3 T. Lopez-Leon, V. Koning, K. B. S. Devaiah, V. Vitelli and A. Fernandez-Nieves, *Nat. Phys.*, 2011, **7**, 391–394.
4 H.-L. Liang, E. Enz, G. Scalia and J. Lagerwall, *Mol. Cryst. Liq. Cryst.*, 2011, **549**, 69–77.
5 H.-W. Liang, Q.-F. Guan, Z. Zhu, L.-T. Song, H.-B. Yao, X. Lei and S.-H. Yu, *NPG Asia Mater*, 2012, **4**, e19.
6 T. Lopez-Leon and A. Fernandez-Nieves, *Phys. Rev. E*, 2009, **79**, 021707.
7 T. Lopez-Leon, A. Fernandez-Nieves, M. Nobili and C. Blanc, *Phys. Rev. Lett.*, 2011, **106**, 247802.
8 H. Liang, J. Noh, R. Zentel, P. Rudquist and J. Lagerwall, *Philos. Transact. A Math. Phys. Eng. Sci.*, 2013, **371**, 20120258.
9 J. Fan, Y. Li, H. Bisoyi, R. Zola, D. Yang, T. Bunning, D. Weitz and Q. Li, *Angew. Chem. (Int. Ed.)*, 2015, **54**, 2160–2164.
10 S. Lee, B. Kim, S. Kim, J. Won, Y. Kim and S. Kim, *Adv. Mater.*, 2015, **27**, 627–633.
11 J. Noh, H.-L. Liang, I. Drevensek-Olenik and J. P. F. Lagerwall, *J. Mater. Chem. C*, 2014, **2**, 806–810.
12 J. Chen, E. Lacaze, E. Brasselet, S. R. Harutyunyan, N. Katsonis and B. L. Feringa, *J. Mater. Chem. C*, 2014, **2**, 8137–8141.
13 J. Noh, I. Drevensek-Olenik, J. Yamamoto and J. P. Lagerwall, *SPIE OPTO, Emerging Liquid Crystal Technologies X*, 2015, **9384**, 93840T–93840T.
14 M. A. Gharbi, D. Sec, T. Lopez-Leon, M. Nobili, M. Ravnik, S. Zumer and C. Blanc, *Soft Matter*, 2013, **9**, 6911–6920.
15 E.-K. Fleischmann, H.-L. Liang, N. Kapernaum, F. Giesselmann, J. P. F. Lagerwall and R. Zentel, *Nat. Commun.*, 2012, **3**, ARTN: 1178.
16 M. Bates, G. Skacej and C. Zannoni, *Soft Matter*, 2010, **6**, 655–663.
17 V. Koning, T. Lopez-Leon, A. Fernandez-Nieves and V. Vitelli, *Soft Matter*, 2013, **9**, 4993–5003.
18 S. Kralj, R. Rosso and G. Virga, Epifanio, *Soft Matter*, 2011, **7**, 670–683.
19 O. Manyuhina and M. Bowick, *International Journal of Non-Linear Mechanics*, 2015.
20 V. Mirantsev, Leonid, M. Sonnet, Andre and G. Virga, Epifanio, *Phys. Rev. E*, 2012, **86**, 020703.
21 G. Napoli and L. Vergori, *Phys. Rev. E*, 2012, **85**, 061701.
22 J. Brake and N. Abbott, *Langmuir*, 2002, **18**, 6101–6109.
23 A. Utada, L. Chu, A. Fernandez-Nieves, D. Link, C. Holtze and D. Weitz, *Mrs Bull*, 2007, **32**, 702–708.
24 C. Bahr, *Phys. Rev. E*, 2006, **73**,.
25 C. C. Ruiz, L. Díaz-López and J. Aguiar, *Journal of Dispersion Science and Technology*, 2008, **29**, 266–273.
26 K. Gupta, Jugal, S. Sivakumar, F. Caruso and L. Abbott, Nicholas, *Angew. Chem. (Int. Ed.)*, 2009, **48**, 1652–1655.
27 I. I. Smalyukh, S. Chernyshuk, B. I. Lev, A. B. Nych, U. Ognysta, V. G. Nazarenko and O. D. Lavrentovich, *Phys. Rev. Lett.*, 2004, **93**,.
28 S. Herminghaus, C. Maass, C. Krüger, S. Thutupalli, L. Goehring and C. Bahr, *Soft Matter*, 2014, **10**, 7008–7022.
29 M. Hara, H. Tenmei, S. Ichikawa, H. Takezoe and A. Fukuda, *Jap. J. Appl. Phys.*, 1985, **24**, L777.